Flow Measurement and Instrumentation 41 (2015) 28–35

Contents lists available at ScienceDirect

Flow Measurement and Instrumentation

journal homepage: www.elsevier.com/locate/flowmeasinst

Improved numerical integration method for flowrate of ultrasonic flowmeter based on Gauss quadrature for non-ideal flow fields

Dandan Zheng [a,*], Dan Zhao [a], Jianqiang Mei [b]

[a] Tianjin Key Laboratory of Process Measurement and Control, School of Electrical Engineering & Automation, Tianjin University, Tianjin 300072, China
[b] Aeronautical Automation College, Civil Aviation University of China, Tianjin 300300, China

ARTICLE INFO

Article history:
Received 17 October 2013
Received in revised form
27 August 2014
Accepted 21 October 2014
Available online 1 November 2014

Keywords:
Multipath ultrasonic flowmeter
Numerical integration method for flowrate
Gauss–Jacobi method
Optimized Weighted Integration for Circular Sections method
Non-ideal flow field

ABSTRACT

Multipath ultrasonic flowmeters with large diameter are widely used in industry. And their measurement performances are sensitive to velocity profiles in conduits. Gauss–Jacobi and Optimized Weighted Integration for Circular Sections (OWICS) method are commonly applied in flow measurement of multipath ultrasonic flowmeters, both of which assume ideal flow in pipes. They are not proper for non-ideal flow measurement. Therefore, an improved numerical integration method for flowrate based on Gauss quadrature is proposed. With this method, optimum relative path heights and corresponding weights are determined according to specific disturbed flows. By comparison Gauss–Jacobi, OWICS with the improved method, the validity of the proposed method is verified for typical disturbed flows based on both theoretical analysis and experiments, and measurement performances of ultrasonic flowmeters are improved significantly.

1. Introduction

Ultrasonic flowmeters have been developing fast in recent years due to its several features, such as no moving parts, non-intrusive, no pressure loss, wide measurement range and high accuracy. Especially, the most prominent advantage is that it can be applied in large diameter measurement while keeping an accurate result. A.G.A Report no. 9 is evidence of the interest that the gas industry has in ultrasonic flowmeters [1]. Besides, the use of multipath acoustic transit time flowmeters has gained acceptance for turbine performance testing and hydroelectric plant optimization in applications world wide [2]. However, limited by spaces and cost, some industrial applications of flow measurement do not have the luxury of long straight pipes thus the flow entering the flowmeter is often distorted, which influences the overall accuracy of ultrasonic flowmeter very strongly. Furthermore, flow calibration (wet calibration) on ultrasonic flowmeter with large diameter is hardly achieved since the limitation of relatively small pipes of standard flow facility, which influence its application. Dry calibration method is regarded as an effective way to solve this problem. However, there is an essential issue need to be studied and resolved in the process of implementation and improvement of the dry calibration method. The shape of the transducer mount (projecting or recessed) has been mentioned in ASME PTC 18-2002 [3]. It is indicated that systematic error due to the above two mounting effects should be included in the measurement uncertainty analysis. Accordingly, measurement performances of ultrasonic flowmeters are affected by both pipe configurations and transducer mounting, which have been studied by researchers.

In 1996–1999, installation effects of three type ultrasonic flowmeters downstream of four typical pipe configurations were studied by NEL [4], including contraction, expansion, single bend and double bend. For all pipe configurations, it was showed that measurement errors of ultrasonic flowmeter with single diametric path are much larger than the meter with dual mid-radius. For example, at 5 diameters (D) position downstream of single bend, the error was about 10% with the single diametric configuration, while only 5% was achieved by the mid-radius configuration. It was indicated that the installation effect was not only a function of the pipe configuration and downstream distance but of the meter design and orientation also. In 2002, pipe configuration effects of the dual mid-radius meter were further tested downstream of a twisted double bend and a twisted tripe bend, respectively [5]. 2% error was still existed at 30*D* downstream distance because of swirl flow. Compared to single path flowmeter, although multipath flowmeter can reduce measurement error to a certain extent, it is still necessary to improve both of their flow adaptabilities to

* Corresponding author. Tel.: +86 13502194892; fax: +86 2227404274.
E-mail address: zhengdandan@tju.edu.cn (D. Zheng).

http://dx.doi.org/10.1016/j.flowmeasinst.2014.10.005
0955-5986/

achieve accurate measurement, especially for complex pipe configurations and shorter downstream distance. Several studies have been carried out. In 2006, the results of testing performed on three different 4-in. multipath ultrasonic flowmeters were reported by NOVA Chemicals Corporation [6]. Meters in fully developed flow and downstream of single elbow and two-elbows-out-of-plane installations, with and without flow conditioning, were tested, respectively. It was concluded that flow conditioning should be used to minimize the amount of metering error. In 2012, because of complex flow fields close to the bend upstream and the turbine inlet downstream, the flowmeter with 18-path configurations were designed for the Three Gorges Project, which was the maximum number of acoustic paths currently used for ultrasonic flowmeters. It was showed that the meter accuracy was better than 1%, which was sufficiently accurate for the turbine performance testing in the Three Gorges Power Station [7].

On the other hand, several studies have been carried out to solve the problem of acoustic transducers mounting effects on measurement. Measurements with 8-path ultrasonic flowmeter were numerically simulated in hydraulic smooth and rough conduits by Voser [8], which indicated that measurement errors due to the transducer protrusion have to be taken into account. The protrusion error was smaller than $\pm 0.5\%$ for diameters larger than 2 m except for velocities below 0.1 m/s. The range of the measurement errors decreased with the increasing diameter. Experimental verification on Voser's conclusions was provided by Lowell [9]. While in the same year, a vortex structure inside transducer cavities was investigated by Loland Lars [10]. Both measurements and numerical simulations of cavity flow were conducted. It was shown that a small vortex was located downstream of the corner while a bigger one was in the lower part of the cavity, which affected the ultrapulse increasing as the pipe flow increased. However, only two-dimensional cavities effects were discussed and the real ultrasonic cavities were not considered. In 2000, transducer cavities in small diameter ultrasonic flowmeter were discussed by Delsing based on computational fluid dynamic (CFD) simulations [11]. It was shown that the recirculation pattern within the cavities was not identical and the cavity influence on the "free stream" flow was different for the up and down stream cavity. Renaldas [12] described a methodology for measurement and experimentally obtained results of local flow velocity components using invasive flow sensors (thermoanemometers) in the transit time ultrasonic flowmeter recesses. It was indicated that the symmetry of flow profile along ultrasonic paths were influenced by recesses and an additional measurement error might occur if calculating the total flowrate not taking into account the local character of the profile distortions. In 2011, CFD modeling approach of the effect on transducer protrusion and recess were discussed by the author [13]. The flow fields for two typical transducer installations were analyzed and the mechanism of both flow effects on measurement accuracy were explained and compared, respectively. It was showed that smaller measurement error could be achieved with protruding transducers, which was a better arrangement type of transducer for ultrasonic flowmeters.

In summary, many works have been done by researchers and flow mechanism was analyzed to help improve measurement performances of ultrasonic flowmeters in non-ideal flow fields. In author's opinion, for multipath ultrasonic flowmeter, numerical integration method for flowrate is important, which determines position of each acoustic path and weighting factor [3]. Three Gaussian quadrature methods were introduced and compared by Thomas [14,15], which are commonly applied in flowmeters. However, Gauss–Legendre quadrature is used for the integration in a rectangular pipe because its weighting function is 1. While for the circular pipe, Gauss–Jacobi method assumes uniform velocity distribution and Optimized Weighted Integration for Circular Sections (OWICS) method assumes fully developed turbulent velocity profile. It is showed that these methods are only proper for undisturbed and symmetrical flow profiles. And errors occur when the actual profile deviates from this.

Therefore, to improve measurement performances of ultrasonic flowmeters in non-ideal flow fields, numerical integration method for flowrate is mainly discussed in this paper. By analysis on problems of commonly used method based on Gaussian quadrature, an improved Gaussian method for flow measurement is proposed. Furthermore, the validity of the improved method is verified by some typical disturbed flows with both theoretical analysis and experiments.

2. Theory of numerical integration method for flowrate based on Gaussian quadrature

2.1. General theory

Numerical quadrature is the numerical calculation of the area below a curve using interpolating polynomials. This corresponds to a numerical integration to calculate a definite integral (from a to b) of function $f(x)$

$$I = \int_a^b f(x)dx \tag{1}$$

The integral I is approximated by a finite number N of known values of $f(x)$ at the known abscissas $x_1, x_2, \ldots, x_N$. The weights $\omega_1, \omega_2, \ldots, \omega_N$ are chosen such that

$$I = \int_a^b f(x)dx \cong \omega_1 \times f(x_1) + \omega_2 \times f(x_2) + \cdots + \omega_N \times f(x_N) \tag{2}$$

Eq. (2) is called N-point quadrature.

The Gaussian quadrature is extended to the numerical integration of the more general type of integrals

$$I = \int_a^b W(x) \times f(x)dx \cong \omega_1 \times f(x_1) + \omega_2 \times f(x_2) + \cdots + \omega_N \times f(x_N) \tag{3}$$

where, $W(x)$ is called the weighting function. The method provides the best numerical estimate of an integral by determining optimum abscissas $x_1, x_2, \ldots, x_N$ and the corresponding weights ω_1, $\omega_2, \ldots, \omega_N$. To find abscissas and weights, procedure of the Gaussian quadrature is introduced below.

Polynomials are generated based on the recurrence

$$\begin{aligned} &P_{-1} = 0 \quad P_0 = 1 \\ &P_{j+1}(x) = (x - a_j) \times P_j(x) - b_j P_{j-1}(x) \\ &j = 0, 1, \ldots, N-1 \end{aligned} \tag{4}$$

where

$$a_j = \frac{\int_a^b W(x) \times x \times p_j^2(x)dx}{\int_a^b W(x) \times p_j^2(x)dx} \quad b_j = \frac{\int_a^b W(x) \times p_j^2(x)dx}{\int_a^b W(x) \times p_{j-1}^2(x)dx}$$
$$j = 1, 2, \ldots, N \tag{5}$$

The abscissas $x_1, x_2, \ldots, x_N$ of the N-point numerical integration are equal to the roots of the polynomial $p_N(x)$ generated by the recurrence of Eq. (4). In order to obtain x_j, the matrix J is constructed.

$$J = \begin{bmatrix} a_0 & \sqrt{b_1} & & & \\ \sqrt{b_1} & a_1 & \sqrt{b_2} & & \\ & \vdots & \vdots & & \\ & & \sqrt{b_{N-2}} & a_{N-2} & \sqrt{b_{N-1}} \\ & & & \sqrt{b_{N-1}} & a_{N-1} \end{bmatrix} \tag{6}$$

x_j is an eigenvalue of the symmetric tridiagonal matrix J when $p_N(x_j)=0$.

Once the abscissas are determined, the weights are computed with the formula

$$\omega_j=\frac{1}{W(x_j)}\int_a^b W(x)\times l_j(x)dx \quad j=1,2,\ldots,N \tag{7}$$

where $l_j(x)$ is the j'th Lagrange Polynomial defined as

$$l_j(x)=\prod_{\substack{k=0\\k\neq j}}^{N}\frac{x-x_k}{x_j-x_k} \tag{8}$$

2.2. Numerical integration method for flowrate of ultrasonic flowmeter

Fig. 1 shows a typical 4-path ultrasonic flowmeter, where L_i denotes path length and φ is path angle. l_i is path length projected on Y–Z-plane. d_i is path position and $\bar{v}_i$ is averaged velocity along path. R is radius of flowmeter. Numerically the flowrate Q can be calculated as

$$Q=\int_{-R}^{R} l(y)\bar{v}(y)dy=\int_{-R}^{R} 2\sqrt{R^2-y^2}\bar{v}(y)dy \tag{9}$$

Define $y=Rt$, and Eq. (9) is transformed as

$$Q=2\int_{-R}^{R}\sqrt{R^2-y^2}\bar{v}(y)dy=2R^2\int_{-1}^{1}\sqrt{1-t^2}\bar{v}(Rt)dt \tag{10}$$

where $\sqrt{1-t^2}\bar{v}(Rt)$ is defined as the area flow function $F(t)$ which describes distribution of partial flowrates on the strips. The basic idea of the numerical integration for flowrate is therefore to approximate the integral by a weighted sum of the given area flow function $F(t)$ at certain heights d_i.

$$Q=2R^2\int_{-1}^{1}F(t)dt\cong\sum_{i=1}^{N}\Delta Q_i=2R^2\sum_{i=1}^{N}\omega_i\times F(t_i) \tag{11}$$

where t_i denotes the relative path height and $t_i=d_i/R \quad t\in[-1,1]$. N is the finite number of measured paths.

Based on the theory of Gaussian quadrature, the weighting function $W(x)$ can be set equal to the area flow function $F(t)$ [14]. Therefore, the optimum relative path height t_i and corresponding weight ω_i can be calculated with Eqs. (4)–(8).

For Gauss–Jacobi method which is commonly applied in multi-path ultrasonic flowmeter, uniform velocity distribution is assumed. So the area flow function is $F(t)=\sqrt{1-t^2}\bar{v}(Rt)$ where $\bar{v}(Rt)=1$. However, in real flows, zero velocity is existed at the wall due to friction. The OWICS method based on turbulent flow profile is presented and $\bar{v}(Rt)=(1-t^2)^{0.1}$.

3. Improvement of Gaussian quadrature based on disturbed flow

According to analysis on Gauss–Jacobi method and OWICS method, both are not proper for disturbed flow measurement. Therefore, an improved method is studied and proposed based on real velocity distributions in conduits.

Step 1: It is important to obtain velocity distributions of disturbed flows. Generally, there are two approaches: One is based on flow pattern models. Several typical distorted flows have been well described by theoretical asymmetric flow profiles proposed by Salami [16]. And some of these flow pattern models have been verified by Frank [17] and Zanker [18] with experiments. The other way is based on CFD simulation, which is proper for any flow. And detailed three-dimensional velocities can be obtained. However, the most significant is to verify the simulation method which can reflect real flow fields.

Step 2: Compute the area flow function $F(t)$. In order to simplify the calculation, $F(t)$ is discreted with $t=-1:0.01:1$, which divides an cross-section of ultrasonic flowmeter into 200 strips as shown in Fig. 2. Therefore, the function is $F(t_g)=\sqrt{1-t_g^2}\bar{v}(Rt_g)$ where $t_g=-1:0.01:1$ and $g=1,2,\ldots,201$. Accordingly, $\bar{v}(Rt_g)$ is calculated as average composition velocity of the gth chord line on the cross-section in consideration of three-dimensional velocities existed in distorted flows.

$\bar{v}(Rt_1)=\bar{v}(Rt_{201})=0$ due to friction at the wall. Then

$$\bar{v}_x(Rt_g)=\tfrac{1}{l_g}\int v_{xg}dl \quad \bar{v}_y(Rt_g)=\tfrac{1}{l_g}\int v_{yg}dl \quad \bar{v}_z(Rt_g)=\tfrac{1}{l_g}\int v_{zg}dl$$

$$\bar{v}(Rt_g)=\bar{v}_x(Rt_g)+\bar{v}_y(Rt_g)\times\frac{y}{x}+\bar{v}_z(Rt_g)\times\frac{z}{x}$$

$$g=2,3,\ldots,200 \tag{12}$$

where, l_g denotes the gth chord length. v_{xg}, v_{yg}, v_{zg} are three-dimensional velocities along the chord which can be obtained

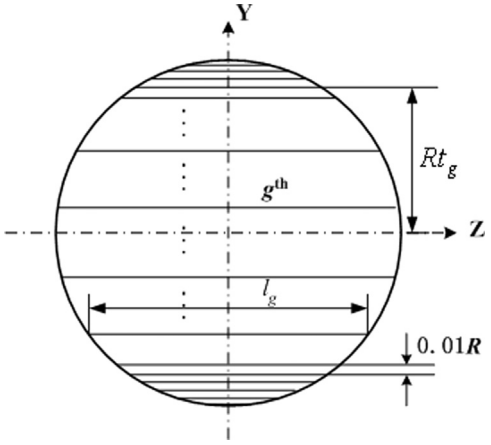

Fig. 2. Cross-section of ultrasonic flowmeter divided into strips.

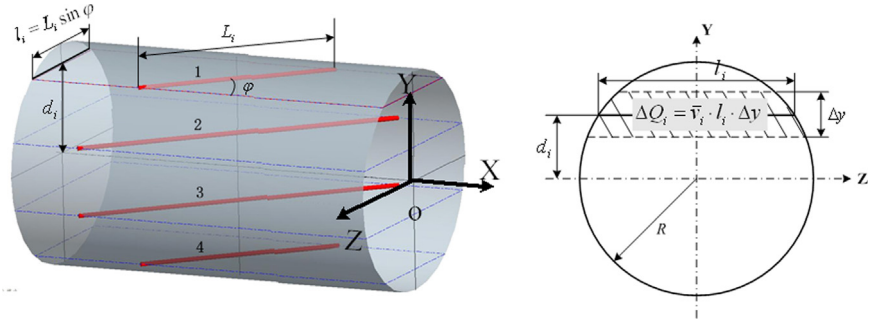

Fig. 1. Schematic of numerical integration for flowrate of ultrasonic flowmeter.

with two approaches mentioned in Step 1. As Eq. (12), it is necessary to translate the transverse flow ($\overline{v}_y$ and $\overline{v}_z$) projected to flow direction X, for which y/x and z/x are coordinate transformations.

Step 3: Once the area flow function $F(t_g)=\sqrt{1-t_g^2}\overline{v}(Rt_g)$ $(g=1,2,\ldots,201)$ is determined, the optimum relative path height t_i and corresponding weight ω_i can be calculated $(i=1,2,\ldots,N)$ for N-path ultrasonic flowmeter. Then Eqs. (4), (5), (7), (8) are transformed to Eqs. (13)–(16), respectively.

$$P_{-1}=0 \quad P_0=1$$
$$P_{j+1}(t_g)=(t_g-a_j)\times P_j(t_g)-b_jP_{j-1}(t_g)$$
$$j=0,1,\ldots,N-1 \tag{13}$$

where

$$a_j=\frac{\sum_{g=1}^{201}F(t_g)\times t_g\times p_j^2(t_g)\times 0.01}{\sum_{g=1}^{201}F(t_g)\times p_j^2(t_g)\times 0.01} \quad b_j=\frac{\sum_{g=1}^{201}F(t_g)\times p_j^2(t_g)\times 0.01}{\sum_{g=1}^{201}F(t_g)\times p_{j-1}^2(t_g)\times 0.01}$$
$$j=1,2,\ldots,N \tag{14}$$

Then t_i are eigenvalues of the symmetric tridiagonal matrix J shown in Eq. (6).

$$\omega_i=\frac{1}{F(t_i)}\sum_{g=1}^{201}F(t_g)\times l_i(t_g)\times 0.01 \tag{15}$$

where

$$l_i(t_g)=\prod_{\substack{k=0\\k\neq i}}^{N}\frac{t_g-t_k}{t_i-t_k} \tag{16}$$

Step 4: Flowrate measured by the N-path ultrasonic flowmeter can be calculated with the optimum t_i and ω_i.

$$Q=2R^2\sum_{i=1}^{N}\omega_i\times F(t_i)=2R^2\sum_{i=1}^{N}\omega_i\times\sqrt{1-t_i^2}\times\overline{v}(Rt_i) \tag{17}$$

It is necessary to mention that the discrete step is 0.01 in this paper, which can be modified according to disturbed flows. The more complex flow is, the smaller step is adopted.

4. Improved method verified based on Salami profiles

In order to verify the proposed numerical integration method for disturbed flow, two typical theoretical velocity profiles are selected among 23 profiles presented by Salami.

$$P1: \quad v(r,\theta)=(1-r)^{1/9}+\frac{2}{\pi^5}r(1-r)^{0.25}\theta^2(2\pi-\theta)^2 \tag{18}$$

$$P2: \quad v(r,\theta)=(1-r)^{1/9}+3.32r(1-r)^2e^{-0.5\theta}\ \sin\ \theta \tag{19}$$

As shown in Eqs. (18) and (19), both models are two-dimensional velocity profiles, where v denotes normalized velocities along flow direction. r is normalized by pipe radius R and $r\in[0,1], \theta\in[0,2\pi]$. It has been suggested that P1 is resembled as the flow downstream of a single bend and P2 is similar with the flow downstream of a double out of plane bend. According to the flow pattern models, profiles are plotted in Fig. 3, which describe the same as results given in reference [19]. Fig. 3a shows profile P1 and Fig. 3b shows profile P2.

Based on two typical profiles, Gauss–Jacobi method, OWICS method and the improved numerical integration method are compared to calculate measurement errors ε with various rotation angles ψ. As shown in Fig. 3, the rotation angle describes separation angle between parallel path line and horizontal axis Z. 2-path and 4-path ultrasonic flowmeters are discussed, respectively.

For Gauss–Jacobi and OWICS method, the relative path height t_i and their weight ω_i are not changeable with various ψ. In contrast, for each rotation angle, optimum t_i and ω_i are determined with the improved method based on specific velocity distributions along 201 chord lines parallel to acoustic paths.

4.1. Comparison results with P1 profile

4.1.1. For 2-path ultrasonic flowmeter

Seven rotation angles are tested in the paper. Tables 1 and 2 show results with Gauss–Jacobi and OWICS method, respectively. Table 3 shows results with the improved numerical integration

Table 1
Results with Gauss–Jacobi method.

ψ (°)	t_1	t_2	ω_1	ω_2	ε(%)
0	−0.5	0.5	0.9069	0.9069	1.986
30	−0.5	0.5	0.9069	0.9069	1.857
60	−0.5	0.5	0.9069	0.9069	1.686
90	−0.5	0.5	0.9069	0.9069	1.636
120	−0.5	0.5	0.9069	0.9069	1.686
150	−0.5	0.5	0.9069	0.9069	1.857
180	−0.5	0.5	0.9069	0.9069	1.986

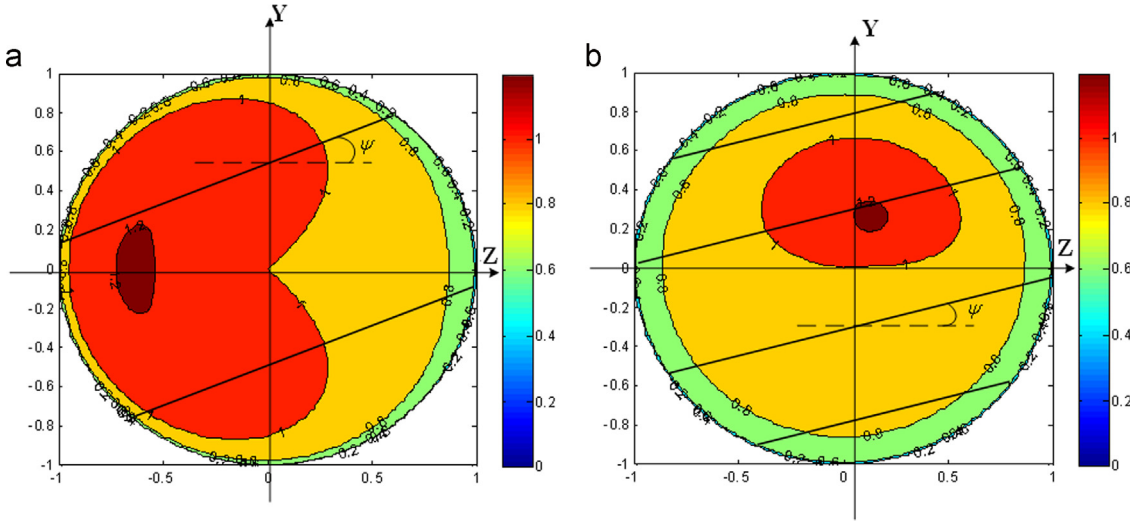

Fig. 3. Salami profiles. (a) Salami profiles P1. (b) Salami profiles P2.

method. Because velocity distribution of P1 is symmetrical to the horizontal axis Z (Fig. 3a), measurement errors are same with both complementary angles, such as 0° and 180°, 30°and 150°and so on. By calculation on the new relative path height t_i and their weight ω_i with the improved method, measurement errors are reduced from 1.6–1.9% (Gauss–Jacobi method) and 0.7–1.0% (OWICS method) to 0.3%. It is indicated that good flow adaptability can be achieved by the improved method.

Table 2
Results with OWICS method.

ψ (°)	t_1	t_2	ω_1	ω_2	ε(%)
0	−0.4880	0.4880	0.8908	0.8908	1.034
30	−0.4880	0.4880	0.8908	0.8908	0.919
60	−0.4880	0.4880	0.8908	0.8908	0.776
90	−0.4880	0.4880	0.8908	0.8908	0.739
120	−0.4880	0.4880	0.8908	0.8908	0.776
150	−0.4880	0.4880	0.8908	0.8908	0.919
180	−0.4880	0.4880	0.8908	0.8908	1.034

Table 3
Results with the improved method.

ψ (°)	t_1	t_2	ω_1	ω_2	ε(%)
0	−0.4891	0.4891	0.8854	0.8854	0.343
30	−0.4773	0.4989	0.9036	0.8689	0.342
60	−0.4668	0.5054	0.9160	0.8576	0.338
90	−0.462	0.5077	0.9196	0.8535	0.335
120	−0.4668	0.5054	0.9160	0.8576	0.338
150	−0.4773	0.4989	0.9036	0.8689	0.342
180	−0.4891	0.4891	0.8854	0.8854	0.343

4.1.2. For 4-path ultrasonic flowmeter

Compared to 2-path ultrasonic flowmeter, 4-path arrangement has much better measurement performance with three methods (as shown in Tables 4–6) because of increasing path line located. Although some measurement errors with the improved method are larger than errors with OWICS method, better stable results with various ψ are obtained.

4.2. Comparison results with P2 profile

Limited by paper space, comparison results of measurement errors for profile P2 are only given in Fig. 4, where horizontal axis is rotation angle ψ and vertical axis is measurement error ε. Fig. 4a and b show results for 2-path and 4-path ultrasonic flowmeter, respectively. It is illustrated that measurement errors are still sensitive to rotation angles for two flowmeters with Gauss–Jacobi and OWICS method, because their relative path height t_i and weight ω_i are not changeable with various ψ. With the improved method, measurement errors are not only reduced but also be stable, which has the best flow adaptability.

Based on analysis of two typical non-ideal flow fields for 2-path and 4-path ultrasonic flowmeters, it is verified that the improved Gaussian quadrature method is effective for disturbed flow

Table 4
Results with Gauss–Jacobi method.

ψ (°)	t_1	t_2	t_3	t_4	ω_1	ω_2	ω_3	ω_4	ε(%)
0	−0.809	−0.309	0.309	0.809	0.3693	0.5976	0.5976	0.3693	0.305
30	−0.809	−0.309	0.309	0.809	0.3693	0.5976	0.5976	0.3693	0.274
60	−0.809	−0.309	0.309	0.809	0.3693	0.5976	0.5976	0.3693	0.252
90	−0.809	−0.309	0.309	0.809	0.3693	0.5976	0.5976	0.3693	0.244
120	−0.809	−0.309	0.309	0.809	0.3693	0.5976	0.5976	0.3693	0.252
150	−0.809	−0.309	0.309	0.809	0.3693	0.5976	0.5976	0.3693	0.274
180	−0.809	−0.309	0.309	0.809	0.3693	0.5976	0.5976	0.3693	0.305

Table 5
Results with OWICS method.

ψ (°)	t_1	t_2	t_3	t_4	ω_1	ω_2	ω_3	ω_4	ε(%)
0	−0.7996	−0.3038	0.3038	0.7996	0.3719	0.5882	0.5882	0.3719	0.156
30	−0.7996	−0.3038	0.3038	0.7996	0.3719	0.5882	0.5882	0.3719	0.127
60	−0.7996	−0.3038	0.3038	0.7996	0.3719	0.5882	0.5882	0.3719	0.108
90	−0.7996	−0.3038	0.3038	0.7996	0.3719	0.5882	0.5882	0.3719	0.101
120	−0.7996	−0.3038	0.3038	0.7996	0.3719	0.5882	0.5882	0.3719	0.108
150	−0.7996	−0.3038	0.3038	0.7996	0.3719	0.5882	0.5882	0.3719	0.127
180	−0.7996	−0.3038	0.3038	0.7996	0.3719	0.5882	0.5882	0.3719	0.156

Table 6
Results with the improved method.

ψ (°)	t_1	t_2	t_3	t_4	ω_1	ω_2	ω_3	ω_4	ε(%)
0	−0.7982	−0.3046	0.3046	0.7982	0.3697	0.5887	0.5887	0.3697	0.143
30	−0.7957	−0.2957	0.3123	0.8003	0.3754	0.5935	0.5833	0.3650	0.142
60	−0.7932	−0.2884	0.3176	0.8017	0.3809	0.5955	0.5793	0.3619	0.141
90	−0.7921	−0.2855	0.3195	0.8022	0.3832	0.5958	0.5778	0.3608	0.140
120	−0.7932	−0.2884	0.3176	0.8017	0.3809	0.5955	0.5793	0.3619	0.141
150	−0.7957	−0.2957	0.3123	0.8003	0.3754	0.5935	0.5833	0.3650	0.142
180	−0.7982	−0.3046	0.3046	0.7982	0.3697	0.5887	0.5887	0.3697	0.143

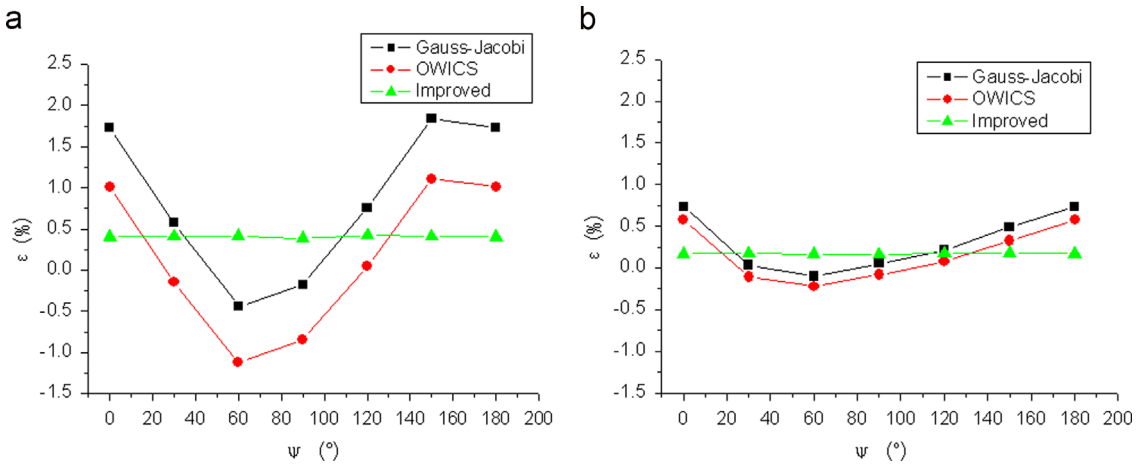

Fig. 4. Comparison results of Gauss–Jacobi, OWICS and the improved method. (a) 2-Path ultrasonic flowmeter. (b) 4-Path ultrasonic flowmeter.

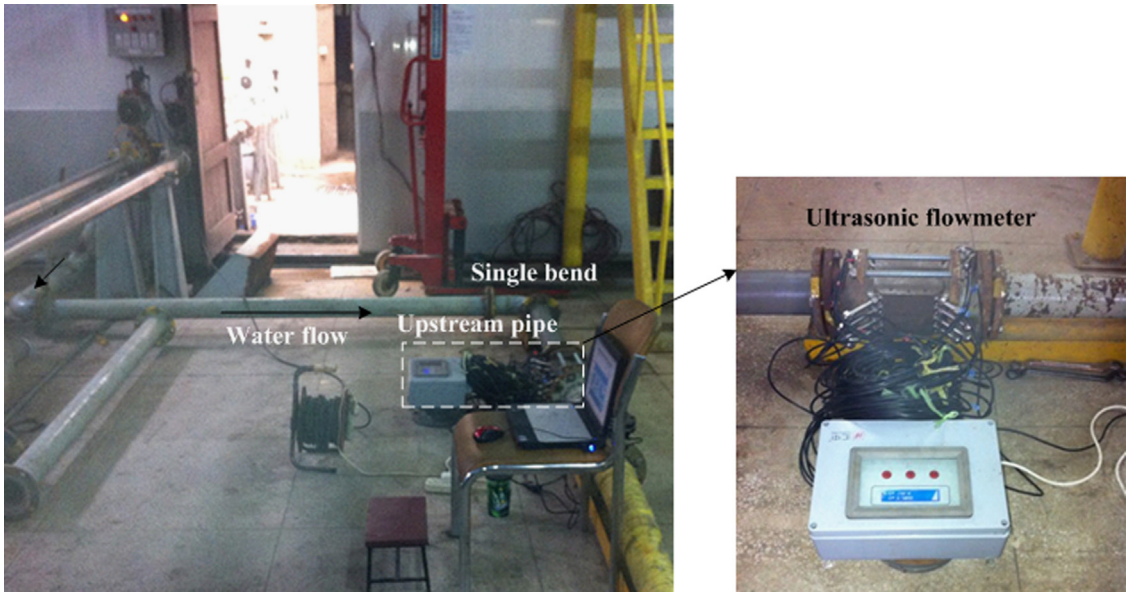

Fig. 5. Experimental photographs.

Table 7
Experimental results with Gauss–Jacobi method.

10*D* downstream of single bend					
u (m/s)	0.296	0.390	1.618	3.386	5.132
ε (%)	−2.887	−3.612	−5.599	−5.587	−5.739
5*D* downstream of single bend					
u (m/s)	0.3	0.359	1.615	3.408	5.157
ε (%)	−4.202	−4.329	−5.957	−6.035	−6.124

Table 8
New weighting factors at 10*D* position.

u (m/s)	ω_1	ω_2	ω_3	ω_4
0.296	0.3959	0.6394	0.6358	0.4074
0.390	0.3987	0.6437	0.6393	0.4035
1.618	0.4068	0.6422	0.6431	0.4055
3.386	0.4050	0.6513	0.6483	0.4036
5.132	0.4041	0.6515	0.6490	0.4032
Average	0.4021	0.6456	0.6431	0.4047

Table 9
New weighting factors at 5*D* position.

u (m/s)	ω_1	ω_2	ω_3	ω_4
0.3	0.3955	0.6517	0.6437	0.3966
0.359	0.3981	0.6529	0.6480	0.3977
1.615	0.4068	0.6444	0.6469	0.4059
3.408	0.4072	0.6460	0.6516	0.4042
5.157	0.4074	0.6442	0.6512	0.4045
Average	0.4030	0.6479	0.6483	0.4018

measurement. The relative path height and their weight are recalculated to specific flow with various rotation angles, which make measurement errors smaller and stable.

5. Improved method verified based on experiments

For actual applications of ultrasonic flowmeter, not only pipe configuration effects but also transducer mounting effects should be considered. To verify the proposed numerical integration method for

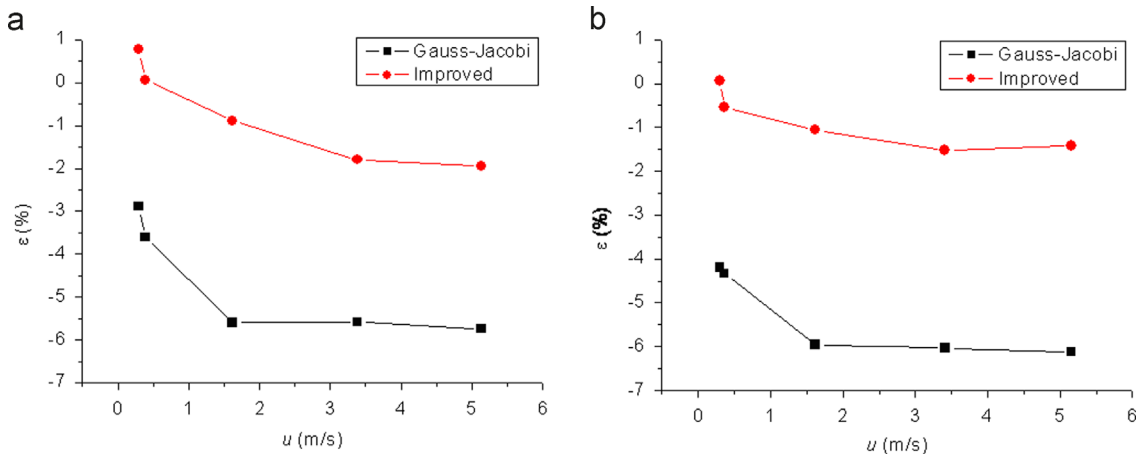

Fig. 6. Comparison results at two tested positions. (a) Results at 10*D* position. (b) Results at 5*D* position.

flowrate, a DN100 8-path ultrasonic flowmeter with protruding transducers is tested downstream of a single bend. Fig. 5 shows pipe configurations and the flowmeter with two cross measurement planes. The diameter D of conduit is 100 mm. The curvature radius of single bend is 150 mm. The length of pipe upstream of single bend is about 30*D*, which assure the flow fully developed.

Path arrangement of the ultrasonic flowmeter is designed according to Gauss–Jacobi method. At each measurement plane, relative path heights t_i are -0.809, -0.309, 0.309, 0.809 and their corresponding path length L_i are 60 mm, 121.047 mm, 121.047 mm, 60 mm. It is necessary to mention that the ultrasonic flowmeter has accurate time of measurement when $L_i \geq 60$ mm. Therefore, 60 mm path length is adopted for paths close to pipe wall, although transducers are not fully protruded into pipe. In order to compare Gauss–Jacobi method and the improved integration method, measurement performances of flowmeter at two positions (10*D* and 5*D* downstream of the single bend) are tested, respectively.

Table 7 shows 10*D* and 5*D* experimental results with Gauss–Jacobi method. Five flow velocities u are tested, which are measured by high accurate electromagnetic flowmeter as a standard meter. ε is measurement error. It is showed that measurement performances of the ultrasonic flowmeter are heavily influenced by both single bend and transducers protrusion. The measurement errors are about -5% in the non-ideal flow fields. To reduce measurement errors, the improved numerical integration method is applied. With this method, the first and significant thing is to obtain three-dimensional velocities in ultrasonic flowmeter. CFD simulation method is adopted, which has been verified by author [13]. Based on three-dimensional velocities on a cross-section of ultrasonic flowmeter, average composition velocity of each chord line is computed with Eq. (12). Then the area flow function is determined for the specific flow. Finally, new weighting factors of each path are calculated based on the old relative path heights, because the ultrasonic flowmeter is not remanufactured. Tables 8 and 9 are new weighting factors at two tested positions with the improved method. It is showed that the weights ω_i have a little difference with various velocities u. In application of ultrasonic flowmeter, it is impossible to change weights with velocities. Therefore, average weighting factors are computed as final weights. Based on the old relative path heights determined by Gauss–Jacobi method and the new weighting factors calculated by the improved method, measurement errors are obtained.

Fig. 6 shows comparison results between Gauss–Jacobi method and the improved method. Fig. 6a illustrates measurement errors at 10*D* position and Fig. 6b is at 5*D* position. The horizontal axis is flow velocity u and the vertical axis is measurement error ε. Although the path heights are not optimized and their corresponding weights are calculated with Eqs. (15) and (16), better measurement performances are still achieved with the improved numerical integration method. Measurement errors are reduced from $-3\sim-6\%$ to $1\sim-1.5\%$. It is further verified that the proposed method is valid for flow measurement in non-ideal flow fields.

It is necessary to mention that there is meaningless to show results with OWICS method in this section, because the path heights determined by Gauss–Jacobi method do not match weights obtained by OWICS method. Only one ultrasonic flowmeter is designed and manufactured.

6. Conclusions

Ultrasonic flowmeters are widely used in industry, and their measurement performances have close relationship with flow fields in conduits. Both pipe configurations and transducers mounting bring about distorted flows, which increase measurement errors. In order to improve measurement, numerical integration method for flowrate based on Gauss quadrature is proposed, which determines optimum relative path height and corresponding weights according to specific velocity distributions of disturbed flows. Two typical theoretical velocity profiles are selected to compare the improved method with Gauss–Jacobi and OWICS method. For both 2-path and 4-path ultrasonic flowmeters, better flow adaptability and measurement accuracy are achieved by the improved method. Furthermore, experiments are carried out to verify the improved method. New weighting factors are determined based on three-dimensional velocities obtained by CFD simulations. Experiment results also show that smaller measurement errors are achieved with the improved method than with Gauss–Jacobi method. Therefore, it is verified that the proposed method is valid for flow measurement in non-ideal flow fields.

Acknowledgments

This paper is supported by the National Natural Science Foundation of China (Grant no. 61101227) and the Natural Science Foundation of Tianjin (Grant no. 13JCQNJC03300).

References

[1] Measurement of gas by multipath ultrasonic meters, American Gas Association. A. G. A. Report no. 9; 1998.

[2] Walsh, JT., A report of acoustic transit time accuracy field work performed in North America. In: Fifth international conference on hydraulic efficiency measurements. Lucerne, Switzerland; July 2004.
[3] Hydraulic turbines and pump-turbines, ASME PTC 18-2002; 2002.
[4] Barton, NA, Brown, GJ. Velocity distribution effects on ultrasonic flowmeters—Part 2 Determination by computational and experimental methods. Report no. 348/99. National Engineering Laboratory; 1999.
[5] Barton, NA, Boam, D. In-service performance of ultrasonic flowmeters—application and validation of CFD modeling methods. Report no. 2002/72. National Engineering Laboratory; 2002.
[6] Mcbrien, Robert, Geerligs, John, Performance of 4-inch ultrasonic meters in high pressure natural gas flow. In: Sixth international symposium on fluid flow measurement; May 2006.
[7] Wang Chi, Meng Tao, Hu He-ming, Zhang Liang. Accuracy of the ultrasonic flow meter used in the hydroturbine intake penstock of the Three Gorges Power Station. Flow Meas Instrum 2012;25:32–9.
[8] Voser, Alex. CFD-Calculations of the protrusion effect and impact on the acoustic discharge measurement accuracy. In: First international conference on hydraulic efficiency measurements. Montreal, Canada; June 1996.
[9] Lowell, Francis, Schafer, Steve, Walsh, Jim. Acoustic flowmeters in circular pipes: acoustic transducer and conduit protrusion effects in discharge measurement. In: Second international conference on hydraulic efficiency measurements. Reno, USA; July 1998.
[10] Loland Lars, Tore, Satran, R., Olsen, Robert. Cavity flow correction for the ultrasonic flowmeter. In: Proc. FLOMEKO. Lund, Schweden; June 1998.
[11] Delsing, Jerker, Niemi, Johan. Ultrasound flow meter errors related to transducer cavities. In: Proc. FLOMEKO. Salvador, Brazil; June 2000.
[12] Raisutis Renaldas. Investigation of the flow velocity profile in a metering section of an invasive ultrasonic flowmeter. Flow Meas Instrum 2006;17:201–6.
[13] Zheng Dandan, Zhang Pengyong, Xu Tianshi. Study of acoustic transducer protrusion and recess effects on ultrasonic flowmeter measurement by numerical simulation. Flow Meas Instrum 2011;22:488–93.
[14] Tresch, Thomas, Grube, Peter. Comparison of integration methods for multipath acoustic discharge measurements. In: Sixth international conference on innovation in hydraulic efficiency measurements. Portland, USA; July 2006.
[15] Tresch, Thomas, Luscher, Bruno. Presentation of optimized integration methods and weighting corrections for the acoustic discharge measurement. In: Seventh international conference on hydraulic efficiency measurements. Milan, Italy; September 2008.
[16] Salami LA. Application of a computer to asymmetric flow measurement in circular pipes. Trans Inst Meas Control 1984;6:197–206.
[17] Frank S, Heilmann C, Siekmann H E. Point-velocity methods for flow-rate measurements in asymmetric pipe flow. Flow Meas Instrum 1996;7:201–9.
[18] Zanker, KJ. The effects of Reynolds number, wall roughness, and profile asymmetry on single-and multi-path ultrasonic meters. In: North Sea flow measurement workshop. Oslo, Norway; October 1999. p. 117–129.
[19] Moore PI, Brown GJ, Stimpson BP. Ultrasonic transit-time flowmeters modeled with theoretical velocity profiles: methodology. Meas Sci Technol 2000;11:1802–11.